8-9-2019

The effect of short and long-term NSAID administration on osteotomy healing in dogs

Hayley Gallaher

The effect of short and long-term NSAID administration on osteotomy healing in dogs

By

Hayley Maloof-Jones Gallaher

A Thesis
Submitted to the Faculty of
Mississippi State University
in Partial Fulfillment of the Requirements
for the Degree of Master of Science
in Veterinary Medical Sciences
in the Department of Clinical Sciences, College of Veterinary Medicine

Mississippi State, Mississippi

August 2019

The effect of short and long-term NSAID administration on osteotomy healing in dogs

By

Hayley Maloof-Jones Gallaher

Approved:

_____

James Ryan Butler
(Major Professor)

_____

Jason Syrcle
(Committee Member)

_____

Erin Brinkman
(Committee Member)

_____

Wes A. Baumgartner
(Committee Member)

_____

Larry Hanson
(Graduate Coordinator)

_____

Stephen B. Pruett
Interim Associate Dean
College of Veterinary Medicine

Name: Hayley Maloof-Jones Gallaher

Date of Degree: August 9, 2019

Institution: Mississippi State University

Major Field: Veterinary Medical Sciences

Major Professor: James Ryan Butler

Title of Study: The effect of short and long-term NSAID administration on osteotomy healing in dogs

Pages in Study 52

Candidate for Degree of Master of Science

The ability of NSAIDs to delay bone healing has been long known, although the extent and exact mechanism remains elusive. The present study evaluates the effect of short duration NSAID on bone healing in dogs following experimental tibial osteotomy. Carprofen was administered twice daily for either 0, 2, or 8 weeks following surgery. Bone healing was evaluated radiographically using RUST scoring at 4 and 8 weeks postop. Postmortem, quantitative CT of for bone mineral density analysis, histologic cartilage:callus ratio of the fracture, and biomechanical testing were performed. Biomechanically, stiffness and maximum stress were higher in dogs that received no carprofen than those that received 8 weeks. Radiographic healing scores were the same for dogs which did not receive carprofen and those receiving a short course, but both were more healed than dogs which received 8 weeks of carprofen. There was no treatment effect on cartilage:callus ratio or bone mineral density.

DEDICATION

I would like to dedicate this research to my daughter, Magdalena, and my husband Aaron- thank you for supporting me while I have pursued by dreams. To my sister Courtney, who has been and continues to be an inspiration, and my parents, for encouraging me in my educational pursuits. Finally, to all the women who came before me and made it possible to come this far.

ACKNOWLEDGEMENTS

I would like firstly to thank Dr. Ryan Butler for being my research mentor and guiding me through grant writing, presentations, and publishing, and pushing me when I didn't know I needed it. I would also like to thank Dr. Jason Syrcle for being such an excellent mentor during my residency training and teaching me so many things. Thank you too to Dr. Steve Elder and Dr. Lauren Priddy for their assistance on the engineering side of things, and to Dr. Robert Wills for his kind and patient statistical expertise throughout this project. I would also like to thank Dr. Cory Fisher for believing in me, and without whom I may never have gotten a surgical residency. Lastly, I would like to thank all my residency siblings: Drs. Paul Vaughn, Andy Law, Allison Kenzig, Jonathan Blakely, and Sarah Castaldo. Thank you for helping me get through these life-altering 3 years and weathering the storm together. Finally, a special thank you to Jamie Walker, TJ Brady, Sarah Heller, and Dr. Alison Lee, for their contributions and technical assistance.

TABLE OF CONTENTS

LIST OF TABLES

LIST OF FIGURES

CHAPTER I

INTRODUCTION

BACKGROUND

Non-steroidal anti-inflammatory drugs' (NSAIDs) ability to inhibit bone healing has been recognized for nearly 40 years (1). Use of NSAIDs for provision of postoperative analgesia for the vast majority of surgical procedures is ubiquitous and considered standard of care in veterinary practice (2). Although the exact mechanism of bone healing inhibition remains unknown, current theories postulate that COX inhibition of prostaglandin synthesis affects the inflammatory phase of healing and leads to an uncoordinated healing response (3, 4).

In the past 25 years, administration of NSAIDs for fracture-related pain relief has come under scrutiny in human medicine as retrospective studies (5-12) identified NSAID administration as a risk factor for delayed union or nonunion in long bone fracture and spinal fusion, while other studies failed to detect an effect of NSAID administration in bone healing (13-15). Resultant literature reviews addressing NSAID use in bone healing approach the issue by one of several methods: 1) offer no specific recommendation on NSAID usage in bone healing (17-19), 2) acknowledge experimental NSAID-induced delays in bone healing in animal models and urge caution in individuals with additional risk factors for delayed healing (19-21), or 3) opine contraindication and avoidance of any and all NSAIDs when fracture healing or spinal fusion is desired (22).

Evidence-based recommendations on NSAID usage during fracture healing are lacking in companion animals, and the reported effects on fracture healing in all species studied have been variable. Decreased fracture healing in rodents and rabbits has been variably assessed using biomechanical strength (23-30), blood flow (31), histology (24, 25, 32), bone density (23, 30, 33), histomorphometry (34-36), rate of non-unions or malunions (27, 28, 32), and radiographic score (26, 27, 32). Two experimental studies in rats (27, 28) detected that NSAID inhibition of fracture healing is dose-dependent, with high doses being more highly inhibitory, mirroring clinical experience in human medicine (11). Other rodent studies which delayed administration of NSAIDs following creation of a fracture documented a lack of negative effects of NSAIDs on bone healing (26, 27). Interestingly, several rodent studies (27, 28, 33, 36) documented that the initial decreases in bone healing seen are reversible once the NSAID is discontinued.

The benefit of NSAID administration in an acute trauma setting should not be underestimated. Prostaglandins induced following induction of COX-2 in immune cells of inflamed tissue propagate inflammation, and contribute to pain hypersensitivity. COX-2 expression is upregulated in painful states to both the peripheral site of injury as well as in neurons of the dorsal horn of the spinal cord (37). Induction of COX-2 in neural cells of the CNS contributes to mechanical pain, such as results from a fracture (38). Thus NSAIDs function as multimodal analgesia with fracture-related pain by both decreasing peripheral inflammation as well as modulating peripheral and central pain sensitization.

In veterinary medicine there is minimal research in companion animals regarding NSAIDs' effects on bone healing utilizing NSAIDs which are FDA approved for use in companion animals. The majority of animal studies which have been performed in veterinary

species have been in rodents and rabbits being used as models for pharmacokinetic and pharmacodynamics studies of NSAIDs which are not approved for use in companion animals. Rather, dosages in the species tested were evaluating toxicity levels, thus doses which wouldn't be standard in those species. Additionally, the fracture models utilized lacked adherence to the principles of fracture fixation as established by the Arbeitsgemeinschaft für Osteosynthesefragen (AO) (39), thus potentially affecting the clinical significance of their findings. This is evidence by the fact that presence of a fracture non-union (28) has been used as an outcome for assessment of fracture healing. A single study performed in dogs (40) documented delayed bone healing in a tibial osteotomy fracture model when long-term administration (12 weeks) of carprofen was compared to no carprofen. However, the clinical relevance of long-term administration of an NSAID in management of patients with fractures is questionable.

BIOLOGY OF BONE HEALING

Bone healing can be described as occurring via one of two processes: primary bone healing and secondary bone healing. The type of healing which occurs is dependent on the type of fracture reduction, the implants' effect on the fracture, amount of strain present across the fracture, and biological environment. In order for primary bone healing to occur, absolute stability must be present where the amount of strain at the fracture site has functionally been eliminated. Thus accomplishing this type of fixation is not possible in the absence of a completely reconstructable fracture.

The goal of fracture healing and fixation can take one of two approaches to either 1) eliminate interfragmentary strain, with goal of creation of absolute stability to provide an environment for primary bone healing, or 2) maintain a low strain environment through bridging

techniques and implants which provides relative stability for secondary bone healing to occur. In order to create an environment for bone healing via secondary bone healing (i.e. endochondral ossification), the osteotomy fracture model used in this study was given a 2mm gap.

Secondary bone healing is a complex biological process, and one of the most remarkable feats of healing within the body, as it heals without forming a fibrous scar, instead completely regenerating the tissue (41). It is the method by which bone healing occurs in nature without stabilization, and involves an organized response from both the periosteum of the bone and the soft tissue capsule surrounding the fracture. It does not require anatomic reduction or rigidly stable conditions; rather, secondary bone healing is enhanced by micromotion and weight-bearing (41, 42). Fractures allowed to heal via secondary bone healing are typically stabilized via interlocking nail, lengthening or bridging plate, external fixation, or with a plate/rod fixation of a complicated, comminuted fracture (42).

Following an initial trauma, the vasculature of the tissues surrounding the bone are disrupted, resulting in hemorrhage. The onset of hemorrhage causes platelet activation and degranulation (44) leading to a release of growth factors and cytokines to the hematoma milieu (42), and ambient hypoxyia induces production of chemotactic factors implicated in cell migration, differentiation, and new bone formation (43). This disruption leads to decreased oxygen tension in the area, as well as reduced nutrients in the local environment. Reduction in oxygen tension acts as a regulatory stimulus for many cells including mesenchymal stem cells (MSCs) and bone progenitor cells (45, 46). Hypoxia-inducible factors (HIFs) are key regulators of the cellular adaptive response to microenvironmental hypoxia, such as seen in a fracture, following disruption of the blood supply, and regulates the expression of multiple genes affecting

cell survival, angiogenesis, and cell metabolism (47). In a hypoxic environment, HIF-α1, which is normally suppressed, accumulates in the nucleus and along with other activation units, regulates expression of downstream target genes including VEGF, SDF-1 and CXCR4 (48-51).

The initial pro-inflammatory response consisting of macrophage infiltration to the site of the injury, has been shown to be vital for endochondral ossification (52). Following macrophage recruitment, T-lymphocytes migrate to the fracture hematoma and initiate the adaptive immune response (53). At the same time, large amounts of pro-inflammatory cytokines are released, namely tumor necrosis factor-α (TNF-α), interleukin-1 (IL-1), IL-6, IL-11, and IL-18 (54-56). These molecules thus create a chemotactic gradient to recruit inflammatory cells and promote angiogenesis (57). The concentration of TNF-α is said to peak within 24-hours post-trauma, and return to baseline within 72 hours (58), during which time it is expressed by macrophages and other inflammatory cells. TNF-α is further believed to mediate an effect by induction of a secondary inflammatory signal and as a chemotactic molecule to recruit necessary cells (59). Of the pro-inflammatory molecules produced, IL-1 and IL-6 are thought to be the most important for fracture healing. The expression of IL-1 and TNF-α overlap in a biphasic mode where macrophages produce IL-1 initially which then induces production of IL-6 by osteoblasts, as well as promoting production of primary cartilaginous callus. IL-1 also promotes angiogenesis at the injured site by activating either of its 2 receptors (57, 59, 60). IL-6, on the other hand, is only present in the acute phase of healing as it stimulates angiogenesis, production of vascular endothelial growth factor (VEGF), and differentiation of osteoblast and osteoclasts from bone progenitor cells (61).

In order for any organ, including bone, to regenerate, MSCs must be recruited, proliferate, and differentiate into their respective progenitor cell; in the case of bone, osteogenic cells. The activation and recruitment of MSCs is multifactorial and incompletely understood. It is has been demonstrated, however, that both local MSCs derived from the damaged tissue, as well as circulating MSCs collaborate in fracture repair and healing (62). Additionally, the biological mechanism is highly regulated by signaling molecules, including growth factors, pro-inflammatory molecules, and angiogenic factors (63).

Platelet-derived growth factors (PDFGs) released from the site of a fracture hematoma have been shown to promote endogenous MSC migration to the fracture site from remote areas of the body in humans (64). Additionally, cytokines produced by macrophages and natural killer (NK) cells can stimulate MSC recruitment (65, 66). Chemokine expression, such as stromal cell-derived factor 1 (SDF-1), are upregulated at the site of injury following a fracture (67). SDF-1 is considered the master regulator for C-X-C chemokine receptor 4 (CXCR4)-positive MSCs, and both contribute to migration of CXCR4 positive MSCs to a fracture site (62, 68), as well as regulating repair activity (68). Evidence of a role for circulating osteogenic progenitor cells' participation in fracture healing has also been demonstrated in a murine model (69). Importantly, it is the initially hypoxic microenvironment (due to disruption of the vascularity surrounding a fracture) which directly contributes to production of chemokines, and recruitment of bone progenitor cells to the site of fracture, which then causes HIF-1α-induced SDF-1 expression that stimulates the migration and homing of circulating CXCR4-positive MSCs (48).

Following the initial formation of a hematoma, a fibrin-rich granulation tissue forms over the fractured end over the course of 7-9 days (41). Although it provides little stability to the

fracture, it is able to withstand higher levels of tension and thus withstand the mobility of the soft tissues inherent following a fracture (42). Simultaneously, intramembranous ossification is occurring subperiosteally, both adjacent to the fracture ends and subperiosteally.

Concurrently with inflammation and continuing during formation of a soft callus and chondrogenesis, intramembranous ossification occurs at between the periosteum and underlying cortex (42). Intramembranous ossification is distinct from endochondral ossification in that MSCs differentiate directly into osteoblasts and begin forming bone without the cartilaginous intermediate. The intramembranous process of bone healing is confined to the fracture between the periosteum and cortex, thus is not sufficient to stabilize the fracture alone. It is visible on radiographs relatively early within the healing process.

With the appearance of a robust bed of granulation tissue, inflammation ends and soft callus formation (chondrogenesis) commences. This granulation tissue consists of endothelial cells, fibroblasts and leukocytes. A provisional extracellular matrix is composed of fibrin, and acts as a temporary scaffold. The matrix, initially, is avascular, and is deposited by fibroblasts and MSC attracted to the area by chemotactic agents within the matrix a cascade of molecular signaling resulting in collagen types I and II. Members of the transforming growth factor beta (TGF-β) superfamily have shown to be of great importance in this process (41). Once MSC are recruited, the matrix continues to remodel and undergo conversion to chondrocytes, i.e. chondrogenesis. Other materials present in the cartilaginous callus include aggrecan, type II cartilage, and other cartilage-specific proteins (42).

For bone regeneration to occur, the soft cartilaginous callus must be transformed into bony callus and later bone. The process of turning cartilage into bone reprises the embryologic

process of endochondral ossification, during which cells proliferate and differentiate, the cell volume increases, and increases in both cell volume and matrix deposition occur (70). The strength of similarity between the embryologic process of endochondral ossification and bone development and generation have been strengthened by identification of a family of molecules, the Wnt-family (71). The Wnt-family is believed to regulate MSCs differentiation into osteoblastic lineage. Additionally, these molecules are thought to regulate bone formation via osteoblasts. Fracture site chondrocytes continue to proliferate and as they do, become hypertrophic and begin to secrete extracellular matrix which calcifies. This process is orchestrated by macrophage colony stimulating factor (M-CSF), receptor activator of nuclear factor kappa B ligand (RANKL), osteoprotegerin (72). TNF-α initiates resorption of the mineralized cartilage, and M-CSF and RANKL. Additionally, genes for collage type II are downregulated and collagen type X are upregulated (72). Collagen type X is specific to endochondral ossification and can be used as a marker for such. In order to make way for matrix calcification, matrix metalloproteinases (MMP) are upregulated to remove the cartilaginous matrix. Vascular ingrowth is also occurring during this phase and requirement of vascular endothelial growth factor (VEGF) during endochondral ossification is well documented (73-75). Induction of VEGF by the hypoxia-inducible factor (HIF) pathway in areas of low oxygen tension has also been documented in the avascular areas of a cartilaginous callus (76). HIF directly increases VEGF transcription as it is a transcription factor VEGF gene expression. Although assuredly hypoxia is one impetus for VEGF production, VEGF has been found to be matrix bound, thus its release via matrix metalloproteinases (MMPs) may be an additional pathway in healing fractures (77).

As the chondrocytes continue to hypertrophy, they eventually undergo apoptosis. Once the mineralization of the cartilage has enough structural strength to attenuate strain to survivable levels for osteoclasts and osteoblasts (42), the advancing osteoclasts remove the mineralized fibrocartilage and deposit osteoid for formation of woven bone. The woven bone, having replaced all hard callus, will completely bridge the callus, and provides and maintains enough rigid structure to resume activity. Radiographically, the bone appears to have a larger diameter and shape may alter from the original appearance of the bone. Over a period of several months to years, the woven bone is converted to lamellar bone with primary and secondary osteons.

EVALUATION OF FRACTURE HEALING

A method to consistently and accurately monitor fracture healing is not currently available in the standard clinical setting. Being able to evaluate the rate and stage of healing is important as this evaluation directs clinical management and ability to bear full weight or return to normal activity in the veterinary patient. It is also helpful in being able to identify fractures that have stalled in their healing sequence and are in a state of delayed or non-union. Equally, evaluation of fracture healing in a research setting should be able to be performed quantitatively in order to facilitate useful studies and effectively evaluate different treatment methods.

The central functional attributes of bones are, 1) their ability to regulate calcium hydroxyapatite mineral deposition and resorption, and 2) the ability to form the microstructure needed to meet the biomechanical load applied by the forces to that bone within the animal (87). Methodologies for evaluation of these two components include imaging, biomechanical testing, serological markers, and observation of clinical improvement.

The existence of a range of modalities to evaluate fracture healing is indicative of the failure of any one modality *alone* to provide sufficient information on fracture healing. Although evaluation of fracture union radiographically is not without fault, it remains the current gold standard for evaluating fracture union in veterinary medicine. The relatively low cost, ubiquity of availability, and familiarity of clinicians with the imaging modality has led to its continued use, in the face of other options.

Considering the widespread use of radiographs to assess bone healing, only limited attempts have been made to establish definitions of radiographic fracture union. Furthermore, use of radiographs for identification of the stage of bone healing has largely been inconclusive (79-81). Research into standardization of radiographic union has been sparse, but within the last 10 years development of two scoring systems by human traumatologists for fractures of the femoral neck via use of the Radiographic Union Score for Hip (RUSH) and tibial fractures, Radiographic Union Score for Tibia (RUST) has come to light (82, 83). The RUST was originally developed for assessment of cortical healing in fractures stabilized with an interlocking nail. In such a situation, because the implant is placed within the medullary canal, two cortices can be visualized on orthogonal views of the affected bone, thus scoring of 4 cortices is achievable in the majority of radiographs. Each cortex is scored for presence or absence of callus, and whether the fracture line is visible or invisible. A score of 1 is awarded when the fracture callus is absent, and fracture line is visible. A 2 is awarded when the callus is present, but fracture line is visible. A 3 is awarded when the callus is present and the fracture line is invisible. Thus, a completely unhealed bone would score a 4/12 and completely healed bone a 12/12. (Figure 1)

Score per cortex	Callus	Fracture Line
1	Absent	Visible
2	Present	Visible
3	Present	Invisible

Figure 1 RUST scoring rubric

RUST score system for radiographic evaluation of fracture healing.

This scoring system requires observation of 4 cortices; this was possible in the tibial fractures stabilized with interlocking nails for which this scoring system was created. When other methods of stabilization are utilized, it is possible that the implant will obscure cortices making a similar scoring system more difficult. In Perlepe et al 2018 (84), it was reported that radiologists' ability to assess cortical healing in plated fractures was significantly reduced (31-56%) compared to those which were stabilized with interlocking nails (90-97%). As such, additional methods for fracture healing evaluation may be desirable in instances of a type of internal fixation besides interlocking nails, particularly in a research setting.

Computed tomography has been shown to have excellent accuracy in determining the bone mineral density of cortical bone. Although dual-energy x-ray absorptiometry (DEXA) was long the standard of care for measurement of bone mineral density and thus osteoporosis in humans, the bone mineral density which can be calculated and extrapolated from quantitative computed tomography (QCT) has been shown to be even more useful than DEXA both in terms of accuracy, as well as prediction of fracture risks. In steroid-induced osteoporosis in

postmenopausal women, bone mineral density of the lumbar spine as measured by QCT, but not by DEXA, was found to be an independent predictor of all types of vertebral fractures (85). Although QCT shows promise for prediction of fractures in patient populations at risk for spontaneous fracture, i.e. in those with decreased bone mineral density to resorption of mineral, use of QCT for fracture healing has not been evaluated to show the same promise. One study (86) evaluated fracture healing assessment methods via 4 different methodologies. Twelve weeks following an experimental tibial osteotomy in dogs, QCT, magnetic resonance imaging, single-photon absorptiometry, and DEXA were performed to evaluate fracture healing as compared to radiographic union. The authors noted that QCT had the best correlation with bone healing of the four modalities; however agreement was still poor. It possible that QCT, although valuable for evaluation of bone mineral density, is poor at evaluating radiographic union due to the inherent heterogeneity and disorganization of bone structure within the period which it would be compared to radiographic union.

In a research setting, biomechanical properties of bone are commonly assessed. Frequently used assessments of these include bending and torsion of bones, as bones experience both of these forces *in vivo*. Tension and compression tests are infrequently used due to the variation within the alignment of fractures, and asymmetry of a fracture callus. Outcomes obtained, regardless of type of test include strength, stiffness, rigidity, and toughness of healing bone. Additionally, non-destructive loads can be used to evaluate the callus and can quantify bending stiffness in multiple planes (87).

Histological examination of bone is another means of evaluating bone healing. Although multiple stains can be used to differentiate tissue phenotype, it is of greatly utility to stain tissue

in such a way to improve and enhance visualization of that tissue by distinguish via distinct coloration from an adjacent and contiguous tissue section. For differentiation of cartilage and bone, Safrinin-O fast green has been widely used, and has been shown to be effective for measuring cartilage thickness in joints with osteoarthritis (88). Regardless of staining protocol, ideally the histological tissue discrimination should be enhanced via the stain chosen.

PATHOPHYSIOLOGY OF PAIN IN FRACTURES

Pain is described as "an unpleasant sensory and emotional experience associated with actual or potential tissue damage, or describe in terms of such damage", by the International Association for the Study of Pain (89). Nociception, on the other hand, is the "neural process of encoding noxious stimuli" (89). It is thus the physiologic process which underlies conscious perception of pain. Unlike with pain, nociception does not require consciousness to occur, and continues even in the presence of general anesthesia if techniques are not employed to block or regulate the transduction, transmission, and modulation (90). Because pain requires conscious awareness, perception is a key aspect of its presence.

At a physiological level, pain begins with presence of a noxious stimulus to sensory neurons. Pain has been associated with bony pathology, including fractures, bone marrow edema syndromes in humans, osteomyelitis, osteoarthritis, and bone cancer (91). Fracture pain, as described by afflicted humans, is a sharp and well-localized pain. It was originally believed that bone pain was not perceived unless the periosteum was involved (92). However, pain is also noted in patients who have bone pathology limited to the bone marrow with no evident periosteal pathology (93). Based on these clinical and experimental observations, it would appear both the periosteum and medullary canal of bones are innervated by primary afferent sensory neurons,

capable of transducing and transmitting nociceptive information (91). Bone pathology has also been noted to produce allodynia and hyperalgesia. These syndromes are consistent with central sensitization of cutaneous afferent neurons and their central projections (94).

With the advent of immunohistochemical markers for neuropeptides, nerve fibers which innervate cortical bone, bone marrow, and periosteum, have been identified as both sensory and autonomic (92, 95-100). The periosteum is innervated by 2 types of neurons: large diameter, fast conducting neurons with encapsulated endings which provide information about non-painful stimulus, and small diameter, slow conducting free fiber endings which are typical of nociceptors (91). The smaller, slow conducting nerve fiber which supply the periosteum are most likely to generate pain associated with mechanical stimulation of the periosteum of bone, i.e. pain associated with fractures. These nerve fibers' conduction velocities and responses to mechanical stimuli suggest roles in both fast, sharp bone pain and slow burning bone pain.

The peripheral afferent sensory neurons have central terminals synapsing with second-order neurons in the dorsal horn of the spinal cord (101). These second-order neurons are either interneurons or projection neurons which then cross to the contralateral side of the spinal cord and carry the signal up the spinal cord, also known as the process of transduction (102). Central sensitization occurs as a result of continued activation or nociception in the periphery, leading to prolonged hyperexcitability of the pain circuits of the central nervous system (CNS) (103). Although the complete mechanisms of central sensitization are multifaceted and complex, COX-2 expression increases significantly locally following initiation of inflammation (104), as well as centrally within the neurons, glia, spinal cord endothelial cells, and brain (104, 105). The release of PGE_2 in the dorsal root ganglion, due to the COX-2 activation peripherally, is essential to the

development of inflammatory hyperalgesia in peripheral tissue (106). The increase in PGE_2 within the CNS following peripheral inflammation is due to the plasticity of the CNS which permits increased spontaneous neuronal activity, reduced activation thresholds, and expansion of the "receptive field", i.e. increased sensitivity to nociception in an area outside the trigger zone, specifically increasing mechanical pain sensitivity (107, 108). These together are manifested as the previously mentioned hyperalgesia (increased sensitivity to noxious stimuli) and allodynia (the interpretation of non-noxious stimulus as pain) seen with fractures.

Because NSAIDs target the source of pain from fractures in the periphery by targeting receptors expressed at the nociceptor peripheral terminals, as well as blocking the sensitizing effect of prostaglandins within the dorsal horn of the spinal cord, NSAIDs as a class of drug can be said to affect central analgesic action in addition to their peripheral action (109). As multimodal analgesia is tenet of modern analgesia, there is a strong argument for administration of NSAIDs in both the pre- and post-operative fracture stabilization period as they can significantly ameliorate the pain associated with the fracture and thus reduce morbidity in the patient.

THEORY OF USE AND PHARMACOKINETICS AND DYNAMICS OF NSAIDS

In the event of injury to a cell, damage to the cell membrane causes release of phospholipids, the most common constituent of the cell membrane. Due to the enzymatic effect of phospholipase A_2 (PLA_2), the previously amphipathic molecules are broken down to arachidonic acid. These molecules are largely recycled back to reform the phospholipid bilayer which make up the eukaryotic cell wall. In the presence of certain stimuli, however, arachidonic acid may be acted upon by cyclo-oxygenase or lipo-oxygenase enzymes to form eicosanoids (i.e.

20-carbon structures) which have various roles in homeostasis and disease. Of those eicosanoids, there are several specific forms which are then transformed and become prostaglandins, prostacyclins, and thromboxane. All of these products act locally and have various immunological and inflammatory roles as well as having important physiological functions. Prostanoid receptors are G-protein coupled receptors which span the cell membrane (110) and classification of 5 subdivisions exist according to the COX metabolite, EP for PGE_2, which when activated leads to further signaling pathways.

Cyclo-oxygenase (COX) enzymes exist in 2 isoforms: COX-1 and COX-2. COX-2 is generally considered an inducible isoform which is present in small amounts in most tissues but which is significantly upregulated in the event of stimulation, such as by pro-inflammatory cytokines, growth factors, and lipopolysaccharide (LPS) found in the outer cell wall of gram negative bacteria, as well as mitogens. COX-2 consists of approximately 600 amino acids, is 70 kDa in weight, and has 60% homology with COX-1 for binding amino acids and NSAIDs (110). Although COX-1 and COX-2 compete for arachidonic acid substrate, COX-2 will preferentially act as the dominant enzyme.

NSAIDs inhibit the biosynthesis of prostaglandins by preventing the substrate arachidonic acid from binding to the COX enzyme active site. NSAIDs usage is ubiquitous in companion animal veterinary medicine, and indeed, amongst all veterinary species. Due to these drugs being uncontrolled or schedule, they are commonly prescribed and dispensed by veterinarians to treat a variety of types of pain. They have both anti-inflammatory and analgesic properties, making them useful, in spite of their profile of side effects and contraindications. Most NSAIDs are now recognized to cause inhibition of both COX-1 and COX-2 enzymes,

depending on NSAID class, but also dependent on species variation. The selectivity of an NSAID for COX-2 vs. COX-1 can be expressed as the COX-1:COX-2 inhibitory ratio, with those with a higher preference for COX-2 being a higher number (111). The published comparisons between non-selective and COX-2 selective NSAIDs varies among drugs used, animal species and study technique used (112, 113). In a 2004 study by Lees et al (110), study results highlighted the differences amongst species and concluded that carprofen, in humans, is relatively COX-1 selective, whereas in dogs and cats carprofen showed preferential activity against COX-2.

REFERENCES

1. Sudmann E and Bang G. Indomethacin-induced inhibition of Haversian remodeling in rabbits. Acta Orthop Scand 1979; 50:621-7

2. Epstein M, Rodan I, Griffenhagen G, et al. 2015 AAHA/AAFP pain management guidelines for dogs and cats. JAAHA 2015; 21:67-84

3. Barry S. Non-steroidal anti-inflammatory drugs inhibit bone healing: a review. Vet Comp Orthop Traumatol. 2010; 6:385-392

4. Blackwell KA, Raisz LG, Pilbeam CC. Prostaglandins in bone: bad cop, good cop? Trends Endocrinol Metab 2010; 21:294-301

5. Hernandez RK, Do TP, Critchlow CW, et al. Patient-related risk factors for fracture-healing complications in the United Kingdom General Practice Research Database. Acta Orthop 2012; 83:653-660

6. Dahners LE and Mullis BH. Effects of nonsteroidal anti-inflammatory drugs on bone formation and soft-tissue healing. J Am Acad Orthop Surg 2004; 12:139-143

7. Bhattacharyya T, Levin R, Vrahas MS, et al. Nonsteroidal anti-inflammatory drugs and nonunion of humeral shaft fractures. Arthritis Rheum 2005; 53(3):364-367

8. Burd T, Hughes M, Anglen J. Heterotopic ossification prophylaxis with indomethacin increases the risk of long-bone nonunion. J Bone Join Surg Br 2003; 85B:700-5

9. Deguchi M, Rapoff AJ, Zdeblick TA. Posterolateral fusion for isthmic spondylolisthesis in adults: analysis of fusion rate and clinical results. J Spinal Disord 1998; 11:459-64

10. Giannoudis PV, MacDonald DA, Matthews SJ, et al. Nonunion of the femoral diaphysis: the influence of reaming and non-steroidal anti-inflammatory drugs. J Bone Joint Surg Br 2000; 82B:655-8

11. Glassman SD, Rose SM, Dimar JR, et al. The effect of postoperative nonsteroidal anti-inflammatory drug administration on spinal fusion. Spine 1998;23:834-8

12. Reuban SS, Ablett D, Kaye R. High dose nonsteroidal anti-inflammatory drugs compromise spinal fusion. Can J Anaesth 2005; 52:506-12

13. Adolphson P, Abbaszadegan H, Jonsson U, et al. No effects of piroxicam on osteopenia and recovery after Colles' fracture. A randomized, double-blind, placebo-controlled, prospective trial. Arch Orthop Trauma Surg 1993; 112:127-130.

14. Bhandari M, Tornetta P, Sprague S, et al. Predictors of reoperation following operative management of fracture of the tibial shaft. J Orthop Trauma 2003; 17:353-61.

15. Reuben SS and Ekman EF. The effect of cyclooxygenase-2 inhibition on analgesia and spinal fusion. J Bone Joint Surg Am 2005; 87A:536-42.

16. Koester MC and Spindler KP. Pharmacologic Agents in Fracture Healing. Clin Sports Med 2006; 25:63-73.

17. Kurmis AP, Kurmis TP, O'Brien JX, et al. The effect of nonsteroidal anti-inflammatory drug administration on acute phase fracture-healing: a review. J Bone Join Surg Am 2012; 94:815-23.

18. van Esch RW, Kool MM, van As S. NSAIDs can have adverse effects on bone healing. Med Hypotheses 2013; 81:343-346.

19. Vuolteenaho K, Moilanen T, and Moilanen E. Non-steroidal anti-inflammatory drugs, cyclooxygenase-2 and the bone healing process. Basic Clin Pharmacol Toxicol 2008; 102:10-14.

20. Radi ZA, and Khan NK. Effects of cyclooxygenase inhibition on bone, tendon, and ligament healing. Inflamm Res 2005; 54:358-366.

21. Pountos I, Georgouli T, Calori GM, et al: Do nonsteroidal anti-inflammatory drugs affect bone healing? A critical analysis. Sci World J 2012; 2012:1-14.

22. Dahners LE, and Mullis BH. Effects of nonsteroidal anti-inflammatory drugs on bone formation and soft-tissue healing. J Am Acad Orthop Surg 2004; 12:139-143.

23. Beck A, Salem K, Krischak G, et al. Influence of diclofenac (group of nonsteroidal anti-inflammatory drugs) on fracture healing. Arch Orthop Trauma Surg 2003;123:324-32.

24. Gerstenfeld LC, Thiede M, Seibert K, et al. Differential inhibition of fracture healing by non-selective and cyclooxygenase-2 selective non-steroidal anti-inflammatory drugs. J Orthop Res 2003;21:670-5.

25. Brown KM, Saunders MM, Kirsch T, et al. Effect of COX-2-specific inhibition on fracture-healing in the rat femur. J Bone Joint Surg Am. 2004; 86A:116-23.

26. Endo K, Sairyo K, Komatsubara S, et al. Cyclooxygenase-2 inhibitor inhibits the fracture healing. J Physiol Anthropol Appl Human Sci 2002; 215:235-8.

27. Gerstenfeld LC, Al-Ghawas M, Alkhiary YM, et al. Selective and nonselective cyclooxygenase-2 inhibitors and experimental fracture-healing. Reversibility of effects after short-term treatment. J Bone Joint Surg Am 2007; 89:114-25.

28. Simon AM, and O'Connor JP. Dose and time-dependent effects of cyclooxygenase-2 inhibition on fracture-healing. J Bone Joint Surg Am 2007; 89-A:500-511.

29. O'Connor JP, Capo JT, Tan V, et al. A comparison of the effects of ibuprofen and rofecoxib on rabbit fibula osteotomy healing. Acta Orthop 2009;80:597-605.

30. Dimmen S, Nordsletten L, Madsen JE: Parecoxib and indomethacin delay early fracture healing: a study in rats. Clin Orthop Relat Res 2009; 467:1992-1999.

31. Murnaghan M, Li G, Marsh DR: Nonsteroidal anti-inflammatory drug-induced fracture nonunion: an inhibition of angiogenesis? J Bone Joint Surg Am 2006; 88:140-147.

32. Leonelli SM, Goldberg BA, Safanda J, et al: Effects of cyclooxygenase-2 inhibitor (rofecoxib) on bone healing. Am J Orthop 2006; 35:79-84.

33. Dimmen S, Nordsletten L, Engebretsen L, et al: Negative effect of parecoxib on bone mineral during fracture healing in rats. Acta Orthop 2008; 79:438-44.

34. Giordano V, Giordano M, Knackfuss IG, et al: Effect of tenoxicam on fracture healing in rat tibiae. Injury 2003; 34:85-94.

35. Goodman SB, Ma T, Mitsunaga L, et al: Temporal effects of a COX-2-selective NSAID on bone ingrowth. J Biomed Mater Res A. 2005; 72:279-87.

36. Krischak GD, Augat P, Sorg T, et al: Effects of diclofenac on periosteal callus maturation in osteotomy healing in an animal model. Arch Orthop Trauma Surg 2007; 127:3-9.

37. Malfait AM, Schnitzer TJ. Towards a mechanism-based approach to pain management in osteoarthritis. Nat Rev Rehumatol 2013; 9:654-664.

38. Vardeh D, Wang D, Costigan M, et al: COX2 in CNS neural cells mediates mechanical inflammatory pain hypersensitivity in mice. J Clin Invest 2009; 119:287-294.

39. Schatzker J: Introduction – AO Philosophy and Principles, in: Rüedi M, (ed): AO Principles of Fracture Management (ed 2). Clavadelerstrasse, Switzerland, AO Publishing, 2005, pp XV-XIX.

40. Ochi H, Hara Y, Asou Y, et al: Effects of long-term administration of carprofen on healing of a tibial osteotomy in dogs. Am J Vet Res 2011; 72:634-641.

41. Marsell R, Einhorn TA. The biology of fracture healing. Injury. 2011;42:551-555.

42. Moreno MR, Zambrano S, Déjardin LM, Saunders BM. Bone biomechanics and fracture biology. In: Johnston SA, Tobias KM, ed. Veterinary Surgery: Small Animal. 2nd ed. St. Louis, MO: Elsevier, Inc; 2018:613-649.

43. Wang X, Wang C, Gou W, et al. The optimal time to inject bone mesenchymal stem cells for fracture healing in a murine model. Stem Cell Res Ther. 2018;9(1):1-10.

44. Hackner SG, DiFazio JM. Bleeding and hemostasis. In: Johnston SA, Tobias KM, ed. Veterinary Surgery: Small Animal. 2nd ed. St. Louis, MO: Elsevier, Inc; 2018:100-127.

45. Genetos DC, Toupadakis CA, Raheja LF, et al. Hypoxia decreases sclerostin expression and increases Wnt signaling in osteoblasts. J Cell Biochem. 110:457-67.

46. Raheja LF, Genetos DC, Yellowley CE. The effect of oxygen tension on the long-term osteogenic differentiation and MMP/TIMP expression of human mesenchymal stem call. Cells Tissues Organs. 191:175-84.

47. Lin W, Xu L, Zwingenberger S, et al. Mesenchymal stem cells homing to improve bone healing. J Orthop Translat. 2017;9:19-27.

48. Ceradini DJ, Kulkarni AR, Callaghan MJ, et al. Progenitor cell trafficking is regulated by hypoxic gradients through HIF-1 induction of SDF-1. Nat Med. 2004;10:858-64.

49. Semenza Gl. Targeting HIF-1 for cancer therapy. Nat Rev Cancer. 2003;3:721-32.

50. Forsythe JA, Jiang BH, Iyer NV, et al. Activation of vascular endothelial growth factor gene transcription by hypoxia-inducible factor 1. Mol Cell Biol 1996;16:4604-13.

51. Liu H, Xue W, Ge G, et al. Hypoxic pre-conditioning advances CXCR4 and CXCR7 expression by activating HIF-1alpha in MSCs. Biochem Biophys Res Comm. 2010;401:509-15.

52. Xing Z, Lu C, Hu D, et al. Multiple role for CCR2 during fracture healing. Dis Model Mech. 2010;3:451-8.

53. Andrew JG, Andrew SM, Freemont AJ, et al. Inflammatory cells in normal human fracture healing. Acta Orthopaed Scand. 1994;65:462-6.

54. Wang Y, Chen X, Cao W, et al. Plasticity of mesenchymal stem cells in immunomodulation: pathological and therapeutic implications. Nat Immunol. 2014;15:1009-16.

55. Claes L, Recknagel S, Ignatius A. Fracture healing under healthy and inflammatory conditions. Nat Rev Rheumatol. 2012;8:133:43.

56. Gerstenfeld LC, Cullinane DM, Barnes GL, et al. Fracture healing as a post-natal developmental process: molecular, spatial, and temporal aspects of its regulation. J Cell Biochem. 2003;88(5):873-84.

57. Sfeir C, Ho L, Doll BA, Azari K, Hollinger JO. Fracture repair. In: Lieberman JR, Friedlaender GE, ed. Bone Regeneration and Repair. 1st ed. Totowa, NJ: Humana Press; 2005:21-44.

58. Villano J, Collins DE, Nemzek JA. Inflammatory response. In: Johnston SA, Tobias KM, ed. Veterinary Surgery: Small Animal. 2nd ed. St. Louis, MO: Elsevier, Inc; 2018:1-15.

59. Kon T, Cho TJ, Aizama T, et al. Expression of osteoprotegerin, receptor activator of NF-kappaB ligand (osteoprotegerin ligand) and related proinflammatory cytokines during fracture healing. J Bone Miner Res. 2001;16(6):1004-14.

60. Lee SK, Lorenzo J. Cytokines regulating osteoclast formation and function. Curr Opin Rheumatol. 2006;18(4):411-8.

61. Yang X, Ricciardi BF, Hernandez-Soria A, et al. Callus mineralization and maturation are delayed during fracture healing in interleukin-6 knock-out mice. Bone. 2007;41(6)928-36.

62. Kitaori T, Ito H, Schwarz EM, et al. Stromal cell-derived factor 1/CXCR4 signaling is critical for the recruitment of mesenchymal stem cells to the fracture site during skeletal repair in a mouse model. Arthritis Rhem. 2009;60:813-23.

63. Peng HR, Usas A, Olshanki A, et al. VEGF improves, whereas sFlt1 inhibits, BMP2-induced bone formation and bone healing through modulation of angiogenesis. J Bone Miner Res. 2005;20:2017-27.

64. Tan HB, Giannoudis PV, Boxall SA, et al. The systemic influence of platelet-derived growth factors on bone marrow mesenchymal stem cells in fracture patients. BMC Med. 2015;13:6.

65. Ren GW, Zhao X, Zhang LY, et al. Inflammatory cytokine-induced intercellular adhesion molecule-1 and vascular cell adhesion molecule-1 in mesenchymal stem cells are critical for immunosuppression. J Immunol. 2010;184:2321-2328.

66. Almeida CR, Vasconcelos DP, Goncalves RM et al. Enhanced mesenchymal stromal cell recruitment via natural killer cells by incorporation of inflammatory signals in biomaterials. J R Soc Interface. 2012;9:261-271.

67. Su P, Tian Y, Yang C, et al. Mesenchymal stem cell migration during bone formation and bone diseases therapy. Int J Mol Sci. 2018;19:E2343.

68. Kucia M, Reca R, Miekus K, et al. Trafficking of normal stem cells and metastasis of cancer stem cells involve similar mechanisms: pivotal role of the SDF-1-CXCR4 axis. Stem Cells. 2005;23:879-94.

69. Kumagai K, Vasanji A, Drazba J, et al. Circulating cells with osteogenic potential are physiologically mobilized into the fracture healing site in parabiotic mice model. J Orthop Res. 2008;26:165-75.

70. Breur GL, VanEnkevort BA, Farnum CE, et al. Linear relationship between the volume of hypertrophic chondrocytes and the rate of longitudinal bone growth in growth plates. J Orthop Res. 1991;9:348-359.

71. Chen Y, Alman BA. Wnt pathway, an essential role in bone regeneration. J Cell Biochem. 2009;106:353-362.

72. Barnes GL, Kostenuik PJ, Gerstenfeld LC, et al. Growth factor regulation of fracture repair. J Bone Miner Res. 1999;14:1805-1815.

73. Gerber HP, Vu TH, Ryan AM, Kowalski J, Werb Z, Ferrara N. VEGF couples hypertrophic cartilage remodeling, ossification and angiogenesis during endochondral bone formation. Nature Medicine. 1999;5(6):623-628.

74. Pfander D, et al. Deletion of Vhlh in chondrocytes reduces cell proliferation and increases matrix deposition during growth plate development. Development. 2004;131(10):2497–508.

75. Street J, et al. Vascular endothelial growth factor stimulates bone repair by promoting angiogenesis and bone turnover. Proc Natl Acad Sci U S A. 2002;99(15):9656–61.

76. Komatsu DE, Hadjiargyrou M. Activation of the transcription factor HIF-1 and its target genes, VEGF, HO-1, iNOS, during fracture repair. Bone. 2004;34(4):680–8.

77. Hankenson KD, Dishowitz M, Gray C, et al. Angiogenesis in Bone Regeneration. Injury. 2011;42: 556–561.

78. Whiley SP. Evaluating fracture healing using digital x-ray image analysis. CME. 2011;29:102-106.

79. Hammer RR, Hammerby S, Lindholm B. Accuracy of radiologic assessment of tibial shaft fracture union in humans. Clin Orthop Relat Res. 1985;199:233-238.

80. Blokhuis TJ, de Bruine JH, Bramer JA, et al. The reliability of plain radiography in experimental fracture healing. Skeletal Radiol. 2001;30:151-156.

81. Davis BJ, Roberts PJ, Moorcroft CI, et al. Reliability of radiographs in defining union of internally fixed fractures. Injury. 2004;35:557-561.

82. Whelan DB, Bhandari M, Stephen D, et al: Development of the radiographic union score for tibial fractures for the assessment of tibial fracture healing after intramedullary fixation. J Trauma. 2010;68:629-32.

83. Chiavaras MM, Bains S, Choudur H, et al: The Radiographic Union Score for Hip (RUSH): the use of a checklist to evaluate hip fracture healing improves agreement between radiologists and orthopedic surgeons. Skeletal Radiol. 2013;42:1079-88.

84. Perlepe V, Omoumi P, Larbi A, et al. Can we assess healing of surgically treated long bone fractures on radiograph? Diagn Interv Imaging. 2018;99:381-386.

85. Rehman Q, Lang T, Modin G, et al. Quantitative computed tomography of the lumbar spine, not dual x-ray absorptiometry, is an independent predictor of prevalent vertebral fractures in postmenopausal women with osteopenia receiving long-term glucocorticoid and hormone-replacement therapy. Arthritis Rheum. 2002;46:1292-1297.

86. Markel MD, Morin RL, Wikenheiser MA, et al: Quantitative CT for the evaluation of bone healing. Calcif Tissue Int 1991; 49:427-432.

87. Morgan EF, De Giacomo A, and Gerstenfeld LC. Overview of fracture healing and its assessment. Methods Mol Biol. 2014;1130:13-31.

88. Hacker SA, Healey RM, Yoshioka M, et al. A methodology for the quantitative assessment of articular cartilage histomorphometry. Osteoarthritis Cartilage. 1997;5:343-355.

89. International Association for the Study of Pain. IASP. [online], https://www.iasp-pain.org

90. Tranquilli WJ, and Grimm KA. Introduction: Use, definitions, history, concepts, classification, and considerations for anesthesia and analgesia. In: Grimm KA, Lamont LA, Tranquilli WJ, Greene SA, and Robertson SA, eds. Veterinary Anesthesia and Analgesia. 5th ed. Ames, IA: John Wiley & Sons, Inc; 2015:3-10.

91. Nencini S, Ivanusic JJ. The physiology of bone pain. How much do we really know? Front Physiol. 2016;7:1-15.

92. Mach DB, Rogers SD, Sabino MC, et al. Origins of skeletal pain: sensory and sympathetic innervation of the mouse femur. Neuroscience. 2002;113:155-66.

93. Arnoldi CC. Intraosseous engorgement-pain syndromes. The pathomechanism of pain. In: Arlet J, and Mazières B, eds. Bone Circulation and Bone Necrosis. 1st ed. Springer-Verlag Berlin Heidelberg. 1990:253-259.

94. Ren K, Dubner R. Central nervous system plasticity and persistent pain. J Orofac Pain. 1999;13:155-163.

95. Duncan CP, and Shim SS. J Edouard Samson Address: the autonomic nerve supply of the bone. An experimental study of the intraosseous adrenergic nervi vasorum in the rabbi. J Bone Joint Surg Br. 1977;59:323-330.

96. Gronblad M, Liesi P, Korkala O, et al. Innervations of human bone periosteum by peptidergic nerves. Anat Rec. 1984;209:297-299.

97. Hohmann EL, Elde RP, Rysavy JA, et al. Innervation of periosteum and bone by sympathetic vasoactive intestinal peptide-containing nerve fibers. Science. 1986;232:868-871.

98. Bjurholm A, Kreicbergs A, Brodin E, et al. Substance P- and CGRP-immunoreactive nerves in bone. Peptides. 1988;9:165-171.

99. Hill EL and Elde R. Calcitonin gene-related peptide-immunoreactive nerve fibers in mandibular periosteum of rat: evidence for primary afferent origin. Neurosci Lett. 1988;85:172-178.

100. Hill EL and Elde R. Distribution of CGRP-, VIP-, D beta H-, SP-, and NPY-immunoreactive nerves in the periosteum of the rat. Cell Tissue Res. 1991;264:469-480.

101. Hall JE. Organization of the nervous system, basic function of synapses, and neurotransmitters. In: Hall JE, ed. Guyton and Hall Textbook of Medical Physiology. 12th ed. Philadelphia, PA: Saunders Elsevier; 2011:543-558.

102. Hall JE. Sensory receptors, neuronal circuits for processing information. In: Hall JE, ed. Guyton and Hall Textbook of Medical Physiology. 12th ed. Philadelphia, PA: Saunders Elsevier; 2011:559-570.

103. Woolf CJ. Central sensitization: implications for the diagnosis and treatment of pain. Pain. 2011;152:S2-S15.

104. Samad TA, Moore KA, Sapirstein A, et al. Interleukin-1beta-mediated induction of Cox-2 in the CNS contributes to inflammatory pain hypersensitivity. Nature. 2001;410:471-475.

105. Laflamme N, Lacroix S, Rivest S. An essential role of interleukin-1beta in mediating NF-kappaB activity and COX-2 transcription in cells of the blood-brain barrier in response to a systemic and localized inflammation but not during endotoxemia. J Neurosci. 1999;19:10923-10930.

106. Araldi D, Farrari LF, Lotufo CM et al. Peripheral inflammatory hyperalgesia depends on the COX increase in the dorsal root ganglion. Proc Natl Acad Sci USA. 2013;110:3603-3608.

107. Vanegas H, Schaible HG. Prostaglandins and cyclooxygenases in the spinal cord. Prog Neurobiol. 2001;64:327-363.

108. Dirig DM, Yaksh TL. Spinal synthesis and release of prostanoids after peripheral injury and inflammation. Adv Exp Med Biol. 1999;469:401-408.

109. Malfait AM, Schnitzer TJ. Towards a mechanism-based approach to pain management in osteoarthritis. Nat Rev Rheumatol. 2013;9:654-664.

110. Lees P, Landon MF, Giraudel J, et al. Pharmacodynamics and pharmacokinetics of nonsteroidal anti-inflammatory drugs in species of veterinary interest. J Vet Pharmacol Ther 2004;27:479-490.

111. Papich MG, and Messenger K. Non-steroidal anti-inflammatory drugs. In: Grimm KA, Lamont LA, Tranquilli WJ, Greene SA, and Robertson SA, eds. Veterinary Anesthesia and Analgesia. 5th ed. Ames, IA: John Wiley & Sons, Inc; 2015:227-243.

112. Papich MG. Pharmacologic considerations for opiate analgesic and nosteroidal anti-inflammatory drugs. Vet Clin North Am Food Anim Pract. 2000;30:815-837.

113. Fox SM. Nonsteroidal anti-inflammatory drugs. In: Carroll GL, ed. Small Animal Anesthesia and Analgesia. Ames, IA: Blackwell Publishing, 2008;143-157.

CHAPTER II

THE EFFECT OF SHORT AND LONG-TERM NSAID ADMINISTRATION ON OSTEOTOMY HEALING IN DOGS

OBJECTIVES

The objective of this study is to identify if short-term administration of carprofen, an FDA approved COX-2 specific NSAID, to dogs with appropriate fracture fixation, given at an appropriate dosage, negatively affects healing 8 weeks postoperatively. Based on clinical impression and personal observation that the majority of patients that receive NSAIDs following a fracture or osteotomy receive only a short duration of NSAIDs (2 weeks or less), we hypothesized there would be no difference between dogs administered carprofen for 14 days postoperatively and those that did not receive carprofen. We further hypothesized that both groups would be different to dogs receiving carprofen for the 8 week duration of the study in biomechanical strength, histopathological analysis of cartilage remaining in the callus, radiographic healing, and bone mineral density.

MATERIALS AND METHODS

ANIMALS

Eighteen purpose-bred, sexually intact adult hound dogs from commercial breeding facilities were used in this study. The size and age of the dogs were controlled to limit variation between groups. The study was performed over 1.5 years with 6 dogs (2 per treatment group)

evaluated at three separate time points. The endpoint of each study corresponded with a terminal educational lab for 4th year veterinary students. The 6 dogs in each group were randomly assigned to one of 3 treatment groups using a list randomizer (https://www.random.org/lists/): no carprofen (0-weeks), carprofen at 2.2 mg/kg orally every 12 hours for 14 days (2-weeks), and carprofen at 2.2 mg/kg orally every 12 hours for the 8 week duration of the study (8-weeks). All dogs had preoperative complete blood count, blood serum chemistry, and heartworm antigen testing performed prior to inclusion in our study. Animal care and use was in accordance with the NIH guidelines for the care and use of laboratory animals and all protocols were approved and strictly overseen by the Institutional Animal Care and Use Committee.

TIBIAL OSTEOTOMY

Food was withheld for the 12 hours prior to surgery. Dogs were pre-medicated with 0.005-0.01 mg/kg of acepromazine and 0.1 mg/kg of hydromorphone intramuscularly [IM], then induced with propofol 2-6 mg/kg intravenously [IV] to effect for endotracheal intubation. Following intubation, femoral and sciatic nerve blocks were performed with bupivacaine 0.5% (1mg/kg) using a Stimpod nerve locating device (Xavant Technology) and 21g 4" Ultrastim2104 needle. Anesthesia was maintained with isoflurane inhalant in oxygen for the duration of the procedure. Radiographs of the left tibia were obtained under anesthesia, prior to surgery. Cefazolin 22 mg/kg IV was administered 30 minutes prior to incision and every 90 minutes of surgery. Cefazolin was discontinued following completion of surgery.

All osteotomies were performed on the left tibiae. A medial approach was made to the tibia, and the center of the tibia was located by measuring the distance between needles within the stifle and tibotarsal joint. A jig was placed on the medial tibia to maintain alignment

following the osteotomy. An oscillating saw (Aesculap, Center Valley, PA) was used to perform a transverse osteotomy under saline irrigation mid-tibia. Following osteotomy, the saw blade was positioned in the osteotomy to maintain a 2mm gap while a pre-contoured 3.5 mm 8-hole, broad DCP plate (Veterinary Orthopedic Implants, St. Augustine, FL) was applied to the medial aspect of the tibia with eight 3.5 mm self-tapping cortical screws placed in standard AO/ASIF fashion. The saw blade and jig were then removed, site was flushed, and the wound closed routinely in 2 layers with an intradermal skin closure. Postoperative radiographs of the left tibia were obtained, dogs were fitted with Elizabethan collars, an adhesive bandage applied (Suresite with Telfa pad), after which dogs were allowed to recover from anesthesia.

POSTOPERATIVE CARE AND MONITORING

Hydromorphone 0.05mg/kg was administered subcutaneously every 4 hours for the first 24-36 hours postop. The morning following surgery, dogs in the 2-week and 8-week carprofen groups began receiving oral carprofen, and all dogs were administered Simplicef (cefpodoxime) 5-10 mg/kg orally every 24 hours for 2 weeks. Oral tramadol (4-6 mg/kg) was administered to all dogs every 12 hours following discontinuation of subcutaneous hydromorphone and was continued for 2 weeks following surgery. Cerenia (maropitant citrate) was administered to dogs showing symptoms of nausea at 1 mg/kg subcutaneously every 24 hours as needed for the first 24 to 48 hours postoperatively. A superficial bandage covering of the incision was maintained for the first 48-72 hours. The dogs were housed in separate runs with 3’5” mesh netting ceilings to minimize jumping and administered their prescribed treatment based on group assignment. E-collars were maintained until their incisions were deemed healed by a veterinarian (HG). During incision healing, dogs were monitored for development of infection defined as either the

presence of swelling of the leg, drainage from the incision, or decreased weight bearing on the operated limb. Antibiotics were initiated empirically based on these clinical signs. At 4 weeks postop, dogs were sedated with butorphanol 0.2 mg/kg IV and dexmeditomidine 5 mcg/kg IV, orthogonal left tibial radiographs were obtained, and dexmeditomidine reversed with equal volume atipamezole IM.

EUTHANASIA AND CT ANALYSIS

At the end of the 8 week study period, the dogs were part of an educational lab, at the conclusion of which they were humanely euthanized while under general anesthesia with pentobarbital IV to effect. Following euthanasia, 8 week postoperative radiographs were performed of the left tibia. The tibial implants were then removed, and computed tomography (CT) of both hind limbs was performed with a phantom (QRM Forearm CT phantom: QRM, Möhrendorf, Germany) for later analysis of bone mineral density. (Figure 1)

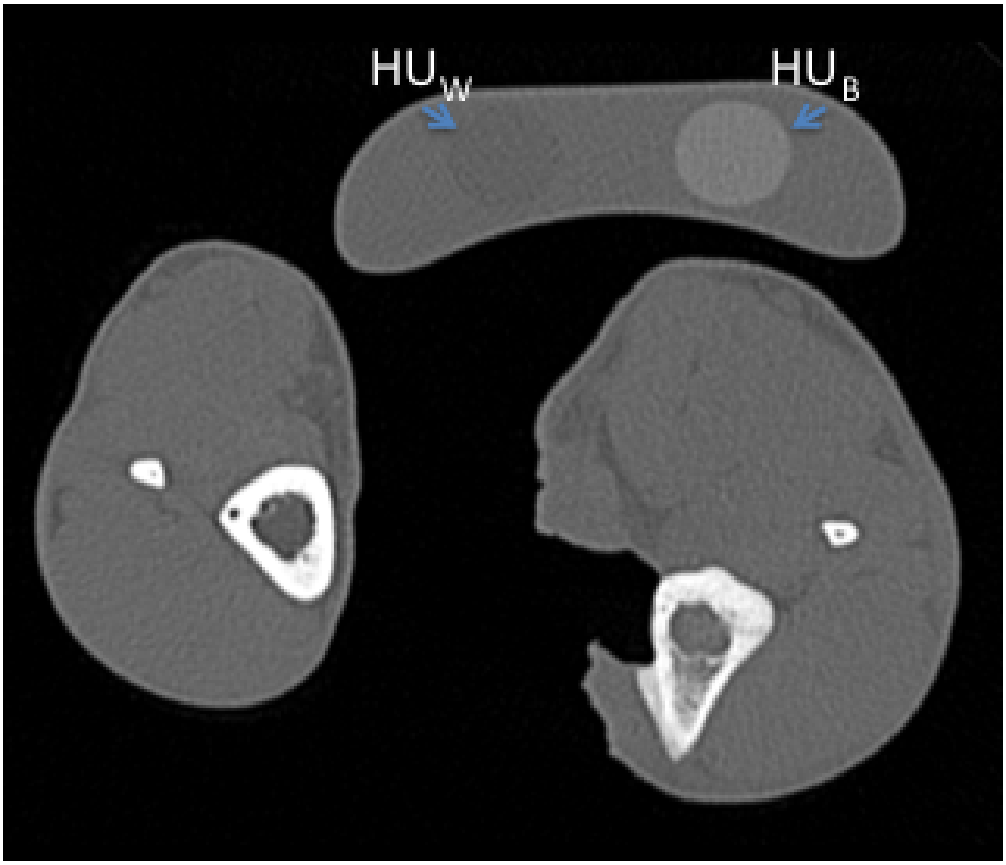

Figure 2 Post-mortem axial CT of tibiae with phantom for BMD calculations.

Axial CT images show both right and left tibiae/fibulae with phantom with known BMD. HU_W = water-equivalent Hounsfield units; HU_B = bone-equivalent Hounsfield units.

BIOMECHANICAL ANALYSIS

The hind limbs were harvested, and the right and left tibiae disarticulated at the stifle, tarsus, and fibula, and were stripped of surrounding muscle and fascia. The specimens were then wrapped in gauze moistened with 0.9% sodium chloride solution, placed in plastic Ziploc bags, and transported on ice to the biomechanical testing facility. Mechanical testing was performed within 2 hours after harvest of specimens. Mechanical testing included non-destructive 3-point

bending tests on all normal and osteotomized tibias. All samples were tested using a universal testing machine (MTI-2K, Measurements Technology, Inc., Marietta, GA) with a 2000 lb. load cell. Experiments were displacement-controlled at a rate of 6 mm/min. Load versus displacement curves were created and the linear region of the curve was identified to determine the stiffness (N/mm) and proportional force limit (N). Stiffness was defined as the slope of the best fit line through the linear region of the curve. The proportional force limit was defined as the maximum force on the linear region of the curve. Proportional force limit (rather than yield or max load) was obtained due to the inherent differences in the failure portion of the curve between normal and osteotomized tibias.

Geometric measurements of the bones were obtained from CT scans taken 8 weeks post operatively following euthanasia of the animals with diameter of the cortex and medullary canal on a sagittal section performed in quadruplicate. The area moment of inertia (AMI, Equation 1) was calculated using CT measurements. In addition to the measurements obtained from load cell testing (stiffness and proportional force limit), the following material properties (i.e., those dependent on geometry) were calculated: maximum stress (Equation 2), elastic modulus (Equation 3), and flexural rigidity (Equation 4) (1).

$$\mathrm{A}MI = \frac{(\pi * \left[\{diameter\ of\ external\ cortex\}^4 - \{diameter\ of\ the\ medullary\ canal\}^4\right])}{64} \quad (1)$$

$$Maximum\ stress = \frac{(0.125 \times maximum\ load\ to\ failure \times distance\ between\ supporting\ points\ on\ the\ shaft \times diameter\ of\ cortex)}{AMI} \quad (2)$$

$$Elastic\ modulus = \frac{stiffness \times (distance\ between\ supporting\ points\ of\ the\ shaft)^3}{48 \times AMI} \quad (3)$$

$$Flexural\ rigidity = Elastic\ modulus \times AMI \quad (4)$$

All values were normalized to those of the contralateral control (intact) tibia to calculate a recovery rate (2). The recovery rate = (osteotomy leg/normal leg)*100.

HISTOLOGY

Bones were placed in 10% buffered formalin solution following biomechanical testing. Once fixed, they were decalcified in Kristensen's solution (formic acid/sodium formate) for approximately 1 month at 25 - 30 degrees Celsius. Samples were then embedded in paraffin and sectioned at 4 microns, then stained with hematoxylin and eosin (H&E) and safranin O-fast green, to highlight remaining cartilage within the bone callus. Each slide was then scanned using a slide scanner (Aperio CS2, Aperio, Ventura, CA). An area 5 mm proximal and 5 mm distal to the original osteotomy was analyzed on sections stained with safranin O-fast green using image analysis software (Aperio ImageScope, Leica Biosystems, Nussloch GmbH, Germany). A cartilage-to-callus ratio was then calculated using a positive pixel count algorithm to calculate strong positive pixels (red and orange, consistent with cartilage) over total pixel area (red and orange plus blue area, representing tissues within the callus, excluding white background). Callus was defined as the tissue at the level of the fracture including fibrous tissue, woven bone, blood vessels and associated nerves. (Figure 2)

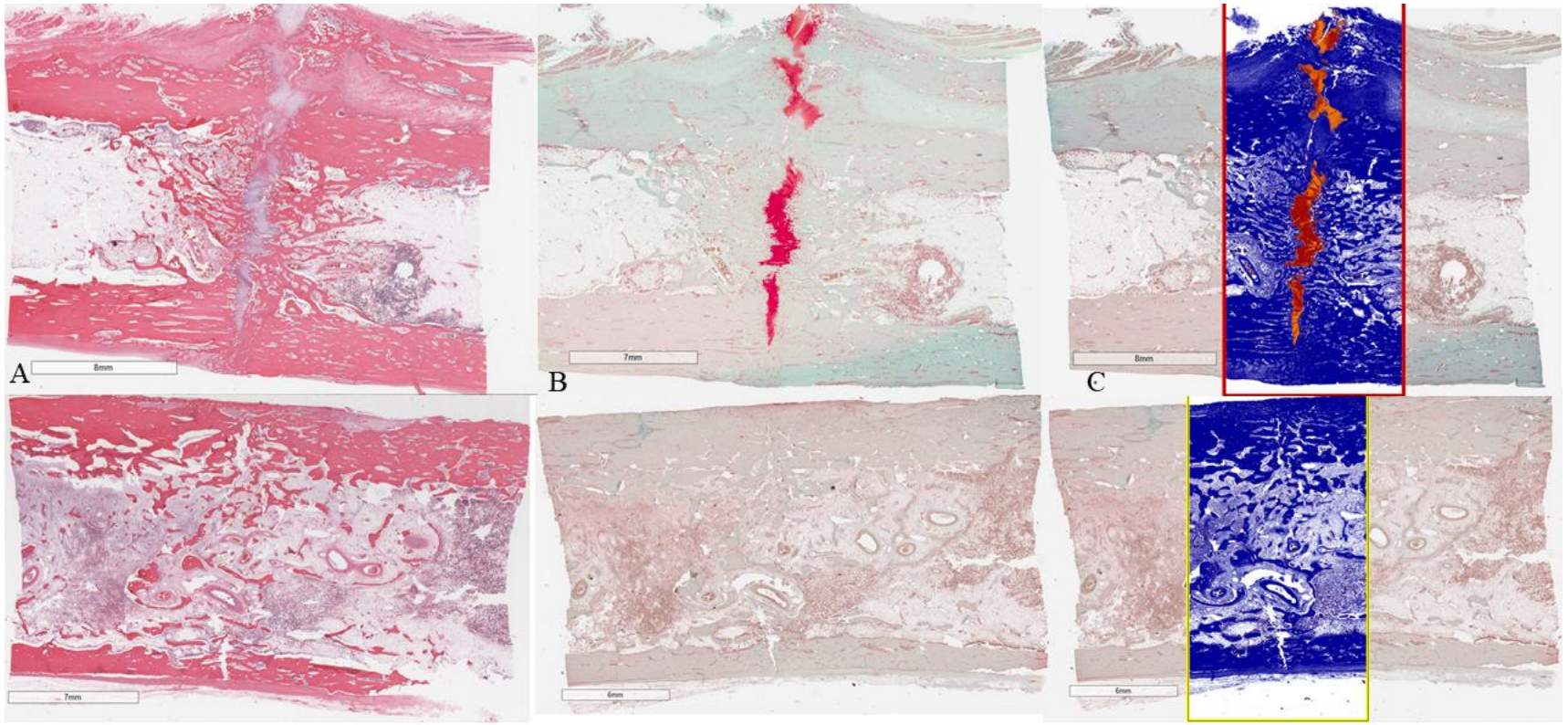

Figure 3 Histologic sections of tibial osteotomy 8 weeks postoperatively.

Slides demonstrate cartilage remaining in callus vs. no callus remaining. Top row: 8-week group. Bottom row: 2-week group. (A) H&E stain of osteotomy section. (B) Safranin-O green (cartilage stains red) (C) Algorithm results for calculation of cartilage : callus ratio. Positive pixel count (red and orange) : total pixel count (dark blue + red and orange).

RADIOGRAPHIC ANALYSIS

Radiographs from 4 and 8 weeks postoperatively were evaluated using the Radiographic Union Scale in Tibial fractures (RUST) scoring system (3). Originally developed and validated for tibial fractures repaired interlocking nails in humans, RUST assesses fracture healing at the 4 cortices on orthogonal radiographic views. Each bone is scored on a 4-12 point scale, summing the score for the 4 cortices. One point is awarded for visible fracture line with no callus, 2 points for visible fracture line with callus, and 3 points for bridging callus with no visible fracture line. Each of the three scorers, a radiologist (EB), surgeon (RB), and surgery resident (HG), were blinded to treatment and study time-point. All scorers were given a written description of the RUST prior to scoring.

QUANTITATIVE CT (QCT) IMAGE ANALYSIS

The post-mortem CT scans of the tibiae were analyzed to obtain the phantom rod pixel values to estimate the water-equivalent Hounsfield units (HU_W) and bone-equivalent Hounsfield units (HU_B). An average pixel value of HU was obtained for cortical bone of normal and osteotomized bone, as well as the callus, at the level of the osteotomy by using three 2mm elliptical regions of interest (ROI). The bone mineral density (BMD) was then estimated using the following formula (Equation 5) as previously described (4).

$$BMD_X = HA_B \times \frac{HU_X - HU_W}{HU_B - HU_W} \quad (5)$$

Where the phantom rod bone density equivalent, $HA_B = 200\ mg/cm^3$ and the measured pixel value from CT is HU_X.

STATISTICAL METHODS

The effect of NSAIDs on measures of biomechanical strength, bone mineral density, histology, and radiographic union score were assessed by generalized linear mixed models using PROC MIXED, SAS for Windows 9.4 (SAS Institute, Inc., Cary, NC). For the measures of biomechanical strength (stiffness, proportional force limit, maximum stress, elastic modulus, and flexural rigidity), the normal tibia, osteotomized tibia values, and recovery rate values were dependent variables in separate models. For bone mineral density, the density of the callus, normal and osteotomized tibia values, and recovery rate values were each analyzed in separate models. A manual forward selection process was followed for variable selection. The model was first fit with only treatment as a fixed effect. The model was then run with either sex, weight, age, or infection as candidate fixed effects in addition to treatment. If one of these additional fixed effects were significant, it was added to the model and the process repeated with each of the remaining candidate fixed effects. Treatment remained in all models regardless of its p-value. Differences in least squares means with Tukey-Kramer adjustment for multiple comparisons were determined for outcomes with a significant fixed effect. For the radiographic union score models, the average of the three observers' scores for each radiograph was used as the dependent variable. For these models, both treatment and time (4 weeks or 8 weeks) were included as fixed effects. Dogs' identity within trial and trial were included as random effects. The variable selection process described above was followed for the radiographic union score model. The distributions of the conditional residuals for all models were evaluated to ensure the assumptions of normality and homoscedasticity had been met for the statistical models. An alpha level of 0.05 was used to determine statistical significance.

Statistical analysis for agreement between the three observers' assessments of radiographic union score was assessed by intra-class correlation (ICC) using PROC MIXED, SAS for Windows 9.4. The ICC is a measure of rating reliability, ranging from 0 to 1, which compares the variability of different scorings of the same radiograph to the total variation across all observers. To assess the agreement among the three observers, an intercept-only model was fit with radiographic union score as the outcome and observer identity and radiograph identity as random effects. The restricted maximum likelihood estimation method was utilized. Covariance parameters from the models were then utilized to calculate the intra-class correlation (ICC) using PROC SQL (5, 6).

RESULTS

DEMOGRAPHICS

A total of 17 of the 18 sexually intact hound dogs completed the study. Eight males and 9 females were enrolled. The mean body weight was 27.65 kg (±4.43). Ages ranged from 8 months at the time of euthanasia to 15 months. The second cohort of dogs were six 6 month old at the start of the study, thus dividing the young dogs evenly amongst study groups. All study groups had 6 dogs with the exception of the 8-week NSAID group, which had 5. One dog was humanely euthanized 8 days post-operatively due to complications associated with a suspected underlying bleeding disorder. A high rate of superficial infection was noted: out of 17 dogs, 10 (58.8%) developed superficial surgical site infections, defined for the purpose of statistical analysis, as dogs which were treatment beyond the perioperative period with antibiotics was initiated on at least one occasion

BIOMECHANICAL TESTING

No biomechanical differences were detected between dogs receiving no carprofen and those receiving 2 weeks of carprofen, or between dogs receiving 2 weeks of carprofen and 8 weeks of carprofen in either osteotomized or normal bones ($p>0.05$). (Table 1)

Table 1 Biomechanical measures and calculations from data obtained 8 weeks post-surgery

Structural Properties						
	0-Weeks	**SD**	**2-Weeks**	**SD**	**8-Weeks**	**SD**
Proportional Force Limit (N)						
Normal Bone (¶, **)	1498.1	284.3	1498.1	275.1	1632.0	250.9
Osteotomy Bone (‡)	751.5	301.4	634.5	226.7	534.5	134.8
Recovery Rate (‡,§)	52.4	25.8	43.1	15.5	33.2	9.0
Stiffness (N/mm)						
Normal Bone	499.7	98.3	471.0	114.1	545.8	134.8
Osteotomy Bone	290.2	70.5	243.5	80.1	222.0	74.6
Recovery Rate (§)	59.6*	16.1	52.7	13.6	42.5*	15.2
Intrinsic Material Properties						
Maximum Stress (MPa)						
Normal Bone	124.9†	9.4	130.9	22.7	141.1†	24.3
Osteotomy Bone	31.8*	12.1	21.2	6.8	17.2*	10.2
Recovery Rate (‡)	25.4*	9.3	16.4	5.2	12.4*	8.0
Elastic Modulus (MPa)						
Normal Bone (†,††, §)	7023.3	1617.5	6978.4	1783.6	7865.7	1628.5
Osteotomy Bone	1735.9	584.2	1179.7	626.9	886.9	667.2
Recovery Rate	24.8	7.2	16.3	6.9	11.9	10.4
Flexural Rigidity (10^6 N/mm)						
Normal Bone	21.3	4.6	20.1	4.9	23.3	5.8
Osteotomy Bone	12.4	3.3	10.4	3.4	9.5	3.2
Recovery Rate (§)	59.6*	17.7	52.7	13.6	42.5*	15.2

Arithmetic means and standard deviation (SD)). Significance is based on differences in least square means from generalized linear mixed models (p-value <0.05), thus numbers below.
(*) Groups differing based on treatment. 0-week > 8-week; no difference was found between 0- and 2-weeks, or 2-weeks and 8-weeks. \
†) Significant only for animals at lower weights (22.5kg, 25kg; not 27.5kg or 30.0kg)
(‡) Infection decreased values.
(§)Younger age increased values/older age had lower values.
(¶) Younger age decreased values
(**) Lower for lighter animals
(††) Females > males

The osteotomized tibias in dogs that received no carprofen recovered more stiffness than those that received carprofen for 8 weeks ($p=0.0351$) when adjusted for age. Younger dogs' osteotomized tibias recovered more stiffness ($p=0.0009$).

Normal tibias of young animals had a lower proportional force limit than those of older dogs ($p=0.0123$). Lighter dogs' normal tibias had a lower proportional force limit of than those of heavier dogs ($p=0.0315$). Regardless of whether dogs received carprofen or not, in osteotomized tibias, infection decreased the proportional force limit ($p=0.024$) and decreased the proportional force limit recovery rate ($p=0.0112$). The osteotomized tibias of older dogs also had a decreased recovery rate of proportional force limit ($p=0.0305$).

The osteotomized tibias of dogs receiving carprofen for 8 weeks were less able to withstand stress ($p=0.0419$), and had decreased recovery rates of maximum stress ($p=0.0140$), compared to those which did not receive carprofen ($p=0.0172$), when adjusted for the occurrence of infection ($p=0.0055$).

Weight and treatment interacted in normal tibias: normal tibias of dogs that received 8 weeks of carprofen had higher maximum stress those which received no carprofen ($p=0.0197$ when assessed for 22.5kg dogs; $p=0.0256$ when assessed for 25kg dogs); this did not hold true when assessed for dogs with higher body weights of 27.5, 30.0, or 32.5 ($p\geq0.1231$). The normal tibias of dogs receiving 8 weeks of carprofen had a lower recovery rate of flexural rigidity than those not receiving carprofen ($p=0.0351$), when adjusted for age ($p=0.0009$). Older dogs had lower recover rates of flexural rigidity in osteotomized tibias. No other treatment effect was noted.

The normal tibias of female dogs had higher elastic moduli than males (p=0.0014). Elastic modulus decreased with increasing age of dogs in normal tibias (p=0.0092).

BONE MINERAL DENSITY (BMD)

Treatment did not affect BMD of normal bone (p=0.7466), osteotomized tibia (p=0.2432), extracortical callus (p=0.0835), or recovery rate of the osteotomized tibia: normal tibia (p=0.5331). Normalized bone mineral density at the osteotomy was not affected by treatment in any of the models. In the normal tibia, BMD was higher in heavier dogs (p=0.0132). Bone mineral density was higher in tibias of older dogs (p=0.0343). (Table 2)

Table 2 Bone mineral density based on calculations from quantitative computed tomography.

Bone Mineral Densities (BMD)						
	0-Weeks	**SD**	**2-Weeks**	**SD**	**8-Weeks**	**SD**
Normal*	1372.9	56.7	1335.8	40.6	1357.8	51.2
Osteotomy †	1000.7	126.3	897.6	87.3	950.1	147.5
Recovery Rate	0.7	0.1	0.7	0.1	0.7	0.1
Callus	768.0	85.6	719.8	146.8	617.8	108.1

(*) = weight is significant. Heavier animals have denser bone.
(†) = age is significant. Older dogs have higher mineral density at the osteotomy.

HISTOLOGY

There was no treatment effect on the cartilage to callus ratio within a 1 cm area around the callus (p=0.2534). (Table 3)

Table 3 Cartilage to callus ratio mean and standard deviation.

Histologic Means of (Cartilage : Callus ratio)*100					
0-Weeks	**SD**	**2-Weeks**	**SD**	**8-Weeks**	**SD**
2.81	3.32	3.02	2.37	5.17	2.14

[(cartilage: callus)*100]. Significance amongst groups is based on differences in least square means from generalized linear mixed models (p-value <0.05). No difference was noted between groups.

RUST (RADIOGRAPHIC UNION SCORE OF THE TIBIA)

The interobserver agreement (ICC) between the 3 scorers was 0.76, which falls in the range of "good" level of agreement.[44,45] No difference in radiographic score was detected between dogs which received no carprofen and those that received 2 weeks of carprofen at either 4 weeks (p=0.9923) or 8 weeks (p=0.9923) postoperatively. (Figure 3) The RUST of both dogs which received no carprofen and those that received 2 weeks of carprofen was greater (i.e. more healed) than that of dogs which received 8 weeks of carprofen at both 4 weeks postoperatively (p=0.0011) and 8-weeks postoperatively (p=0.0011). (Table 4)

Table 4 Mean of RUST and standard deviation.

Mean of RUST by Group and Time Point						
	0-Weeks	**SD**	**2-Weeks**	**SD**	**8-Weeks**	**SD**
4 Weeks	8.67*	1.61	7.33*	1.24	6.40 †	1.06
8 Weeks	10.72*	1.32	10.67*	1.19	8.60 †	0.91

Means and standard deviations of RUST data. In effect, the extent of healing in the 0-week and 2-week groups was greater than that of the 8-week group.
* = No difference between groups. (4 week, p=0.068; 8 weeks, p=0.9860)
† = Less healed compared to * groups.

DISCUSSION

Evaluation of RUST scores for determination of radiographic healing would lead us to accept our hypothesis that there is no difference in fracture healing between dogs given no NSAIDs and a 2-week course of NSAIDs, and that both were more healed than dogs receiving 8 weeks of carprofen. However, only some of the biomechanical testing results (stiffness recovery rate, maximum stress, and maximum stress recovery rate) were consistent with the radiographic findings, with no difference detected of other biomechanical measures between treatment groups. Moreover, the histological appearance and bone mineral density of the callus showed no difference between any of the treatment groups, all of which would cause use to reject our secondary hypothesis. Due to these seemingly differing results, we must examine the stages of bone healing where NSAIDs may be most influential, and whether our test parameters are sensitive enough to adequately assess bone healing 8 weeks postoperatively in the dog.

The exact point at which bone healing is affected by NSAIDs has not been fully elucidated. In our study, the first time point at which objective evaluation was performed was 4 weeks postoperatively. Given that no difference in radiographic healing scores was detected between dogs who did not receive carprofen and those who received 2 weeks of carprofen, but both were more healed than dogs who received 8 weeks of carprofen at 4 weeks postoperatively, it may reasonably be presumed that a difference of 2 weeks of administration of NSAIDs is sufficient both to delay healing as well as to reverse a delay in healing. In one previous study (7), prostaglandin E2 (PGE2) levels within the fracture callus were elevated in rats during the first 2 weeks following a fracture, then tapered after 14 days. Early elevation in PGE indicates a role in bone healing. The same study (7) detected with administration of either a non-specific or COX-2 specific NSAID for 7 days, PGE2 levels rebounded higher than in control rats 14 days after

initial fracture, thus further validating a role of PGE2 during the early phases of bone healing. The role of COX-2 was examined by Zhang et al (8) using genetic knock-out mice lacking COX-1 and COX-2 gene expression: decreased fracture healing 21 days post fracture was detected in the COX-2 knockout mice, while wild-type mice were similar to those lacking COX-1. Furthermore, cell-culture-raised bone marrow stromal cells lacking COX-2 had a 50% decrease in the number and area of bone nodules compared to either COX-1 deficient or wild-type cells. Finally, the addition of PGE-2 or bone morphogenetic protein-2 to COX-2 deficient bone marrow stromal cell culture returned bone area and numbers of nodules to the same as wild type, all of which are consistent with bone metalloproteinases being downstream to PGE-2 and PGE-2 (and therefore COX-2) being necessary for bone formation.

In our dogs, the 2 mm fracture gap was designed to model endochondral ossification. In endochondral ossification, mesenchymal cells first differentiate into chondrocytes, which subsequently undergo terminal differentiation and apoptosis, leading to calcification of the matrix (9). Endochondral bone formation is dependent upon osteoblast differentiation from osteoprogenitor cells (MSCs). In a tibial fracture model of mice lacking COX-2 genes (8), reduced osteoblastogenesis in diaphyseal fractures was noted. This finding was supportive of a critical requirement of COX-2 for mesenchymal stem cell differentiation which is, in turn, a crucial step in endochondral ossification. Lack of mesenchymal stem cell proliferation due to COX-2 selective NSAID administration may be partially responsible for decreased endochondral ossification noted in other studies (2), and a lower RUST score at 4 weeks and 8 weeks postoperatively in dogs that received 8 weeks of carprofen in our study. Histologically, our model failed to document this difference using a more objective cartilage: callus ratio than one

previously described (2). Biomechanically, however, our data are consistent with incomplete bony union causing decreased maximum stress in osteotomized tibias of dogs that received 8 weeks of carprofen. A lack of MSC proliferation may partially explain the difference in biomechanical properties of bone noted in dogs receiving long-term NSAIDs.

Consistent with the previous study in dogs (2), long-term administration of carprofen negatively affected radiographic fracture healing of the tibia in our study using the RUST scoring system. The RUST was created by physicians (3) to improve the reliability of traumatologists' fracture healing assessment and has shown substantial ICC of 0.86 (95% CI 0.79-0.91) and high intraobserver reliability (ICC, 0.88; 95% CI, 0.80-0.96). A recently published report (10) in human medical literature aimed to determine radiologists' ability to assess healing of surgically treated long bone fractures on radiographs found that fracture edges were only seen in only 71% to 81% of the 560 cortical segments evaluated. Furthermore, radiographic union scores could only be calculated in 58% to 75% of fractures. Scoring was significantly less frequently calculable in plated (31-56%) than in fractures stabilized with interlocking nails (90-97%). In our study, the RUST system was used by 3 observers examining radiographs of 17 dogs' tibias at 2 different time points postoperatively. In spite of RUST originally being designed for evaluation of human tibial fractures repaired with interlocking nails, the agreement between observers in plated dog tibias was also high (ICC 0.76). In all radiographs of osteotomized tibias that we evaluated, only 4 out of 34 radiographs had one cortex which was not visible, (i.e. 4 cortices out of 136 examined, or 2.9% of all cortices evaluated). For those cortices, a score was estimated based on callus appearance caudal to the plate. In spite of the RUST scoring system being used

differently than originally intended and not validated for use in dogs, it allowed for a quantitative and repeatable assessment of radiographic union in this study.

The variability in the effect of short-term administration of carprofen on biomechanical properties detected in our study is consistent with previous reports (7, 11). Gerstenfeld et al (7) showed in rats that NSAIDs had no effect on torsional strength (torque to failure), but that shear modulus was decreased by long-term NSAIDs. Though 3-point bending rather than torque to failure was evaluated in our study, long-term NSAIDs affected only some biomechanical assessments of bone strength in our study as well. It is possible that either the variation within groups was too large, the differences between groups were too small to observe, or there were too few dogs per group to reach significance (type II error). For those measure for which no significance was detected between groups, the difference between least squares means for treatment and a 95% confidence interval was calculated (Table 5).

Table 5 Differences and 95% confidence intervals for the least squares means

Differences and 95% confidence intervals for the least squares means				
	P-value	**0-Weeks vs 2-Weeks**	**0-Weeks vs. 8-Weeks**	**2-Weeks vs. 8-Weeks**
Stiffness Normal Tibia	0.5097	28.7 (-71.2 to 128.5)	29.0 (-134.4 to 76.4)	-57.7 (-163.0 to 47.7)
Stiffness Osteotomized Tibia	0.2126	46.7 (-36.7 to 130.1)	74.1 (-13.8 to 162.0)	27.5 (-60.4 to 115.4)
Proportional Force Limit Normal Tibia	0.3725	-0.03 (-213.22 to 213.17)	-133.1 (-359.0 to 92.8)	-133.1 (-359.0 to 92.8)
Proportional Force Limit Osteotomized Tibia	0.3008	74.2 (-175.74 to 324.18)	193.17 (-67.4 to 453.7)	118.95 (-141.1 to 379.0)
Maximum Stress of Normal Tibia	0.3696	-6.0417 (-25.7 to 13.6)	-13.8870 (-34.6 to 6.8)	-7.8452 (-25.5 to 12.8)
Elastic Modulus of Normal Tibia	0.6169	44.8939 (-1387.2 to 1476.9)	-582.87 (-2092.4 to 926.6)	-627.76 (-2137.2 to 881.7)
Elastic Modulus of Osteotomized Tibia	0.1099	556.26 (-228.75 to 1341.3)	849.02 (25.7 to 1672.3)	292.76 (-530.6 to 1116.1)
Flexural Rigidity of Normal Tibia	0.5097	1223624 (-3037531 to 5484780)	-1237107 (-733958 to 3259744)	-2460731 (-6957582 to 2036120)
Flexural Rigidity of Osteotomized Tibia	0.2126	1991981 (-1566966 to 5550928)	3163578 (-587405 to 6914561)	1171597 (-259386 to 4922580)

Differences and 95% confidence intervals for the least squares means of the treatment groups where a significant difference between treatment groups was not detected for biomechanical measures.

No change in conclusions were reached following these calculations. In human medicine, inability to perform *antemortem* biomechanical testing as well as limitations of radiography as a sole gauge of fracture healing has led to development of more objective methods of fracture evaluation. One such example is an implantable strain sensor which is placed across a healing

fracture (12). This device was created to be used adjunctively with radiographic union assessment for evaluation of fracture healing.

Using the RUST, no difference was detected between healing of osteotomized tibias in dogs receiving no carprofen and those that received 2 weeks of carprofen at either 4 or 8 weeks postoperatively. Due to the complexity and thus heterogeneity of a fracture callus, we posited bone healing analysis could be improved using QCT to examine the bone mineral density and thus quantify endochondral ossification at the fracture callus. However, no treatment effect was observed on bone mineral density of the fracture callus. This may imply the stage of bone healing captured 8 weeks postoperatively is not affected by delays in bone healing due to carprofen. In humans, however, QCT is used more commonly as an estimate of bone mineral density for identification of bones at risk for fracture (i.e. osteoporosis) than for bone healing (13). A study (14) evaluating fracture healing 12 weeks post-osteotomy in dogs with QCT, magnetic resonance imaging, single-photon absorptiometry, and dual-energy x-ray absorptiometry, noted that QCT had the best correlation with bone healing of the four modalities; however agreement was still poor (R^2=0.6). Thus, QCT for bone mineral density appears a poor measure of bone healing when compared with radiographic union.

No effect of carprofen administration was detected with the cartilage to callus ratio in our fracture model 8 weeks postoperatively. This conflicts with other studies where greater cartilage content was noted in mice following a COX-2 specific inhibitor (7), and in dogs with long-term administration of carprofen 12 weeks postoperatively (2). However, length of time between fracture and evaluation [27] and longer-term administration of carprofen (2) may explain difference in outcome. Furthermore, because the previous definition of fracture callus was more subjective

(2), interpretation of the cartilage : callus ratio and direct comparison with this study should be avoided.

Limitations of this study include population variation due to sex, age, weight, and superficial infection rate. Within our statistical model, these variants were accounted for so as to minimize the effect on differences detected due to treatment within our 3 groups. (Table 1) Further limitations include the small sample size and the simplified fracture model as it relates to clinical relevance.

Based our findings, a short course of NSAIDs administered in the perioperative period appear to be safe for fracture healing, but should be stopped following a 1-2 week course until the fracture or osteotomy is healed radiographically. This is of particular relevance for patients who receive NSAIDs chronically for management of arthritis undergo fracture repair or osteotomy procedures, such as TPLO or TTA. Cessation of NSAIDs following the immediate postoperative period should be strongly considered in light of the findings of this study.

REFERENCES

1. Manabe T, Mori S, Mashiba T, et al: Human parathyroid hormone (1-34) accelerates natural fracture healing process in the femoral osteotomy model of cynomolgus monkeys. *Bone* 2007; 40:1475–1482

2. Ochi H, Hara Y, Asou Y, et al: Effects of long-term administration of carprofen on healing of a tibial osteotomy in dogs. *Am J Vet Res* 2011; 72:634-641

3. Whelan DB, Bhandari M, Stephen D, et al: Development of the radiographic union score for tibial fractures for the assessment of tibial fracture healing after intramedullary fixation. *J Trauma* 2010; 68:629-32

4. Vaughn DP, Syrcle JA, Ball JE, et al: Pullout strength of monocortical and bicortical screws in metaphyseal and diaphyseal regions of the canine humerus. *Vet Comp Orthop Traumatol* 2016; 29:466-474

5. Maki, Ellen: Interclass reliability in healthcare studies: calculating the intraclass correlation coefficient (ICC) in SAS, in SAS User Group Presentations (ed). (www.sas.com), 2014, accessed 08/09/17.

6. Koo TK, Li MY: A guideline of selecting and reporting intraclass correlation coefficients for reliability research. *J Chiropr Med* 2016; 15:155–163

7. Gerstenfeld LC, Al-Ghawas M, Alkhiary YM, et al: Selective and nonselective cyclooxygenase-2 inhibitors and experimental fracture-healing. Reversibility of effects after short-term treatment. *J Bone Joint Surg Am* 2007; 89:114-25

8. Zhang X, Schwarz EM, Young DA, et al: Cyclooxygenase-2 regulates mesenchymal cell differentiation into the osteoblast lineage and is critically involved in bone repair. *J Clin Invest* 2002; 109:1405–1415

9. Marsell R, Einhorn TA: The biology of fracture healing. *Injury* 2011; 42:551-555

10. Perlepe V, Omoumi P, Larbi A, et al: Can we assess healing of surgically treated long bone fractures on radiograph? Diagn Interv Imaging. 2018;99:381-386

11. Simon AM and O'Connor JP: Dose and time-dependent effects of cyclooxygenase-2 inhibition on fracture-healing. *J Bone Joint Surg Am* 2007; 89-A:500-511

12. Pelham H, Benza D, Millhouse PW, et al: Implantable strain sensor to monitor fracture healing with standard radiography. *Sci Rep* 2017;7:1-8

13. Khoo BC, Brown K, Cann C, et al: Comparison of QCT-derived and DXA-derived areal bone mineral density and T scores. *Osteoporos Int* 2009; 20:1539-45

14. Markel MD, Morin RL, Wikenheiser MA, et al: Quantitative CT for the evaluation of bone healing. *Calcif Tissue Int* 1991; 49:427-432

CHAPTER III

CONCLUSION

Short-term administration of carprofen to dogs following fracture repair results in no delay in radiographic healing; however, long-term administration decreased biomechanical strength and radiographic healing of the tibial osteotomy. Histological evaluation of cartilage within the fracture callus and bone mineral density of the fracture callus were inadequate assessments of bone healing 8-weeks post-osteotomy in our model. Given the desirable effects of NSAIDs following trauma and minimal measurable adverse effects at 8 weeks post-operatively, short-term administration of carprofen in dogs appears safe for fractures that lack other risk factors for delayed healing. Longer duration of administration of NSAIDs following fracture repair should be avoided to prevent delays in bone healing.